

Spectroscopic analysis of the B/Be visual binary HR 1847[★]

J. Kubát¹, S. M. Saad², A. Kawka¹, M. I. Nouh², L. Iliev³, K. Uytterhoeven⁴, D. Korčáková¹, P. Hadrava⁵, P. Škoda¹,
V. Votruba^{1,6}, M. Dovčiak⁵, M. Šlechta¹

¹ Astronomický ústav, Akademie věd České republiky, CZ-251 65 Ondřejov, Czech Republic

² National Research Institute of Astronomy and Geophysics, 11421 Helwan, Cairo, Egypt

³ Institute of Astronomy, Bulgarian Academy of Sciences, 72 Tsarigradsko Shossee Blvd., BG-1784 Sofia, Bulgaria

⁴ Laboratoire AIM, CEA/DSM-CNRS-Université Paris Diderot, CEA, IRFU, SAp, Centre de Saclay, F-91191 Gif-sur-Yvette, France

⁵ Astronomický ústav, Akademie věd České republiky, Boční II 1401, CZ-141 31 Praha 4, Czech Republic

⁶ Ústav teoretické fyziky a astrofyziky PFF MU, Kotlářská 2, CZ-611 37 Brno, Czech Republic

draft version November 6, 2021

ABSTRACT

We studied both components of a slightly overlooked visual binary HR 1847 spectroscopically to determine its basic physical and orbital parameters. Basic stellar parameters were determined by comparing synthetic spectra to the observed echelle spectra, which cover both the optical and near-IR regions. New observations of this system used the Ondřejov and Rozhen 2-m telescopes and their coudé spectrographs. Radial velocities from individual spectra were measured and then analysed with the code FOTEL to determine orbital parameters. The spectroscopic orbit of HR 1847A is presented for the first time. It is a single-lined spectroscopic binary with a B-type primary, a period of 719.79 days, and a highly eccentric orbit with $e = 0.7$. We confirmed that HR 1847B is a Be star. Its $H\alpha$ emission significantly decreased from 2003 to 2008. Both components have a spectral type B7–8 and luminosity class IV–V.

Key words. Stars: binaries – stars: Be – stars: individual: HR 1847

1. Introduction

HR 1847 (HD 36408, BD +16°794, HIP 25950, ADS 4131) is a bright visual binary consisting of two B type stars. Throughout this paper, the component at $\alpha(J2000) = 05\ 32\ 14.14$, $\delta(J2000) = +17\ 03\ 29.3$ will be denoted as HR 1847A (or component A) and the one at $\alpha(J2000) = 05\ 32\ 14.56$, $\delta(J2000) = +17\ 03\ 21.8$ as HR 1847B (or component B). The first observations of this binary, which were obtained on 31 December 1782, were reported by William Herschel (see Herschel, 1785, star III.93). He observed this binary again on 21 January 1800 (see Herschel, 1821, star 124).

Although this visual binary consists of two bright stars and Plaskett (1919) recommended further observations, it was not studied much during the last century. Since HR 1847 is both an X-ray source (Berghöfer, Schmitt, & Cassinelli, 1996) and an IRAS source (Coté & Waters, 1987), and considering its brightness, lack of observations, and sometimes confusing catalogue information, it has become quite an interesting object for more detailed study.

2. Summary of known properties of HR 1847

In this section we summarize the information currently available for both components of HR 1847, which is scattered throughout the astronomical literature, online catalogues, and databases.

Send offprint requests to: J. Kubát,
e-mail: kubat@sunstel.asu.cas.cz

[★] Based on observations with the Ondřejov and Rozhen 2-m telescopes.

2.1. Multiplicity

2.1.1. Angular separation

Angular separation ρ and relative position θ of the components of HR 1847 have already been measured by Friedrich Georg Wilhelm Struve (1837, star No. 730) as an average of 4 measurements obtained in 1829 and 1832 ($\rho = 9''.81$, $\theta = 141^\circ.82$). Later measurements resulted in $\rho = 9''.53$, $\theta = 140^\circ.2$ (Cannon, 1912b), $\rho = 9''.7$, $\theta = 140^\circ.9$ (Russell & Moore, 1929), $\rho = 9''.65$, $\theta = 140^\circ.85$ (Perryman et al., 1997, from HIPPARCOS), $\rho = 9''.65 \pm 0''.006$, $\theta = 140^\circ.5$ (Fabricius et al., 2002, from the Tycho catalogue), $\rho = 9''.61$, $\theta = 140^\circ.8$ (Mason et al., 2004, from speckle interferometry). The angular separation, as reported by Lindroos (1983) and Abt & Cardona (1984) is $9''.6$.

2.1.2. Radial velocity variations

The first radial velocity measurements for both components were reported by Plaskett & Young (1919) and they showed variability. Plaskett et al. (1920) suggested that both components are spectroscopic binaries. Frost et al. (1926) designated HR 1847A (No. 126 in his Table II) as a spectroscopic binary with an unknown orbit using only one spectrum secured at the Dominion Astrophysical Observatory (DAO) in 1919 by Otto Struve. Component A was also reported to be a spectroscopic binary by Gahm, Ahlin, & Lindroos (1983) and Abt, Levato, & Grosso (2002). However, no attempt has been made to determine the orbital parameters until now.

Table 1. HIPPARCOS and *UBVRIJHK* photometry of HR 1847.

band	HR 1847A	HR 1847B	source
	mag	mag	
H_p	6.088 ± 0.007	6.455 ± 0.010	HIPPARCOS
B_T	6.036 ± 0.008	6.468 ± 0.004	HIPPARCOS
V_T	6.057 ± 0.009	6.458 ± 0.004	HIPPARCOS
U	5.823 ± 0.030	6.337 ± 0.030	EXPORT
B	6.103 ± 0.037	6.527 ± 0.037	EXPORT
	6.070 ± 0.020	6.520 ± 0.020	Maidanak
V	6.090 ± 0.100	6.490 ± 0.077	EXPORT
	6.090 ± 0.020	6.510 ± 0.020	Maidanak
R	6.037 ± 0.100	6.410 ± 0.077	EXPORT
	6.050 ± 0.020	6.460 ± 0.020	Maidanak
I	6.050 ± 0.150	6.437 ± 0.133	EXPORT
J	5.964 ± 0.019	6.280 ± 0.024	2MASS
H	6.022 ± 0.021	6.275 ± 0.021	2MASS
K	6.016 ± 0.027	6.282 ± 0.016	2MASS

HIPPARCOS – Perryman et al. (1997), EXPORT – Oudmaijer et al. (2001), Maidanak – Shatskii (1998), 2MASS – Skrutskie et al. (2006).

2.2. Distance

The HIPPARCOS parallax of HR 1847 is 2.92 ± 1.57 mas (Perryman et al., 1997), which corresponds to a distance of 342 ± 184 pc, but the large error reduces the reliability of this distance estimate. However, the new edition of the HIPPARCOS catalogue (van Leeuwen, 2007) gives a parallax value of 1.09 ± 2.04 mas, which is unable to provide any information about the distance owing to the very uncertain parallax. Individual parallax measurements of the A and B components are not available.

2.3. Magnitudes and photometry

The first reliable magnitude values ($V_A = 6.07$, $V_B = 6.44$) were published by Cannon (1912b). She also gives the combined AB magnitude as 5.49. Maybe that only the combined magnitude value was given in her earlier spectral classification (Cannon, 1912a) and in the HD catalogue (Cannon & Pickering, 1918) caused its being incorrectly but often quoted as the magnitude of the A component until now. A similar value is also listed in the Bright Star Catalogue ($V = 5.46$, Hoffleit & Jaschek, 1991).

The photometry of HR 1847 was measured by several authors always during observing runs devoted to large sample of stars. Eggen (1977) measured *uvby* photometry of early type stars and derived values $V_A = 6.1$ and $V_B = 6.5$. Lindroos (1983) measured *uvby* photometry of visual binaries including HR 1847. He derived corresponding V magnitudes of both components from the y filter values as $V_A = 6.091 \pm 0.019$ and $V_B = 6.510 \pm 0.023$. *BVR* observations of visual binaries at Mount Maidanak were performed by Shatskii (1998), and he obtained $V_A = 6.09 \pm 0.02$ and $V_B = 6.51 \pm 0.02$. The EXPORT *UBVRI* photometry (observed by the Nordic Optical Telescope, Oudmaijer et al., 2001) gave values $V_A = 6.09 \pm 0.10$ and $V_B = 6.49 \pm 0.07$. Recent determinations of magnitudes were derived from HIPPARCOS photometry (see Perryman et al., 1997). With the HIPPARCOS V_T and B_T magnitudes, Kharchenko (2001) derived the magnitudes $V_A = 6.056 \pm 0.008$ and $V_B = 6.451 \pm 0.004$, which do not differ too much from the first values of Cannon. A more complete list of photometric magnitudes of both components of HR 1847 is given in Table 1.

2.4. Polarization

Oudmaijer et al. (2001) found the value of V band polarization $P_V = 0.0063 \pm 0.0004$ for the A component, and $P_V = 0.0063 \pm 0.0002$ for the B component.

2.5. Spectral types and luminosity classes

The early classification of both components was ‘*egregie alba*’ (very white) by Struve (1837). Later, (Cannon, 1912b) classified both stars as B9.

Using his own observations in the period from April 1954 to March 1955 at the Yerkes Observatory, Osawa (1959) determined the spectral type of component A as B7IV and of component B as B8IV. From his own observations with the Perkins telescope, Slettebak (1963) determined spectral types B7III for component A and B7IV for component B. Cowley et al. (1969) determined spectral types B8III and B8V for components A and B, respectively, using spectra from MacDonald and Yerkes Observatories. Levato (1975) observed both components at Cerro Tololo Inter-American Observatory and obtained spectral type B7III for component A and B8IV for B. Finally, Mora et al. (2001) changed the Bright Star Catalogue classification of HR 1847A from B7IIIe to B5V.

2.5.1. Emission

Andrews (1968) found that component B shows $H\alpha$ emission using $H\alpha$ photometry, which was later spectroscopically confirmed by Wackerling (1970). The emission sign, which appeared at the spectral type of component A in both the Bright Star Catalogue and the Simbad database, is incorrect, as $H\alpha$ emission was never reported for HR 1847A.

2.6. Rotation

Rotational velocities of both components were first determined by Slettebak (1963). The projected rotational velocity of component A was measured as $(v \sin i)_A = 50 \text{ km s}^{-1}$, while component B was found to be rotating rapidly, $(v \sin i)_B = 300 \text{ km s}^{-1}$. Levato (1975) determined $(v \sin i)_A = 60 \text{ km s}^{-1}$ and $(v \sin i)_B = 300 \text{ km s}^{-1}$. Abt et al. (2002) refined the values of the rotational velocities to $(v \sin i)_A = 45 \text{ km s}^{-1}$ and $(v \sin i)_B = 200 \text{ km s}^{-1}$ using coude spectra obtained at the Kitt Peak 0.9-m telescope.

2.7. Variability

Slightly different values of magnitude obtained at different times using different instruments, which are listed in the Section 2.3, cannot be considered as firm proof of variability. The only available homogeneous set of observations was obtained by the HIPPARCOS satellite. Using HIPPARCOS photometry, Percy, Harlow, & Wu (2004) determined the characteristic time scale of variability for HR 1847 as 0.9 days. They conclude that it is a classical Be star, but it is not clear which component they are referring to, since both components A and B have HIPPARCOS photometry available. In addition, data for both components also include several values that correspond to the combined magnitude of both components. Since it is not clear that they excluded the apparently wrong values (those corresponding to combined A+B magnitude), their result is questionable. We performed an independent search for variability and could not confirm the variability time scale found by Percy et al. (2004).

2.8. X-rays

HR 1847 has also been identified as an X-ray source by ROSAT (Berghöfer et al., 1996) with an X-ray luminosity $\log L_X = 29.64$ (in the paper version). In the online version of the same catalogue (their Table 2), this value is slightly different, $\log L_X = 29.79$. Both corresponding values of $\log(L_X/L_{\text{bol}}) = -6.82$ (or -6.79 in the online version) correspond to a typical $\log(L_X/L_{\text{bol}})$ relation for B-type X-ray emitters (cf. Berghöfer et al., 1997). It is, of course, a question of which star of the pair is the X-ray source, if not both. The position of the ROSAT source 1RXS J053214.9+170319 suggests it is more probably coincident with the star TYC 1301-1942-1=HR 1847B (Flesch & Hardcastle, 2004); however, the positional error is $18''$ (Voges et al., 2000), so HR 1847A also lies within the error circle.

2.9. IR excess

In their study of IR excess of 101 Be stars Coté & Waters (1987) found IRAS magnitudes $[12] = 4.95$, $[25] = 2.22$, $[60] = -0.92$, which places HR 1847 in the $[12]-[25]/[12]-[60]$ colour-colour diagram far away from the region where almost all Be stars are located. Coté & Waters suggest there is a reflection nebula close to HR 1847. Whitelock et al. (1989) associate HR 1847 with the IRAS SSSC source X0501+589. Magnier et al. (1999) suggest that HR 1847 is a good candidate for a Herbig Ae/Be star with a very large or a very cool circumstellar disk, but Iwata et al. (1999) did not find any CO emission for this star.

Again, it is not clear which star has IR excess, but most likely it is component B, which was found to be a Be star. There is also a small possibility that both stars are Be stars, with component A not in emission at that moment. Further observations may shed a light on it. Coté & Waters (1987) attributed the spectral type B7IIIe to HR 1847, which corresponds to component B, and $v \sin i = 55 \text{ km s}^{-1}$, which corresponds to component A.

2.10. Cluster membership

Although HR 1847 is located in the same region as the open cluster Collinder 65 (A component is #771, B component #772, according to the WEBDA¹ database), its membership is improbable mainly because to the different proper motion (Kharchenko et al., 2004).

3. Observations and data reduction

The data available for this study consist of several data sets of electronic spectra mostly centred on the $H\alpha$ region:

Component A

- 68 spectra in the spectral range 6250–6770 Å obtained with a CCD SITe ST-005 800×2000 pix camera attached to the coudé spectrograph of the 2m-telescope in Ondřejov (Czech Republic). The spectra were obtained between 18 October 2003 and 25 February 2008. Spectra were reduced using IRAF².

¹ The Galactic and Magellanic Clouds open cluster database WEBDA is available at <http://obswww.unige.ch/webda/>

² IRAF is distributed by the National Optical Astronomy Observatories, which are operated by the Association of Universities for Research in Astronomy, Inc., under cooperative agreement with the National Science Foundation.

- One spectrum obtained on 22 March 2003 with the red (5850–8450 Å) and blue (3800–5650 Å) channels of the fiber-fed echelle spectrograph *HEROS* (resolving power ~ 20000 , for its brief description see Kaufer, 1998). The spectrograph was attached to the Cassegrain focus of the 2m-telescope at the Ondřejov Observatory. All the basic data reduction processing was done using the *HEROS* pipeline written by Otmar Stahl and Andreas Kaufer as an extension of the basic MIDAS echelle context (see Stahl et al., 1995, also Škoda & Šlechta, 2002).
- 14 spectra obtained in the spectral range (6510–6608 Å) at Rozhen Observatory (Bulgaria) using the coudé-spectrograph of the 2m RCC telescope. The CCD camera Photometrics AT200 with an SITe SI003AB 1024x1024 CCD chip (24x24 μm pixel size) was used in the f/9.5 camera of the spectrograph to provide spectra with a spectral resolution of 36000 in the $H\alpha$ region. Spectra were obtained between 24 October 2004 and 30 August 2007 and reduced with the MIDAS package.
- One spectrum in the spectral range 6290–6745 Å obtained at Observatório do Pico dos Dias (OPD, Brasil) and published by Vieira et al. (2004). For details and information about the reduction process, see the reference above.

In addition to the electronic spectra, we also used the radial velocity measurements of Plaskett & Young (1919). For comparison purposes, several values of published radial velocities were used from the works of Frost et al. (1926) and Duflot et al. (1992).

Component B spectra came from the same instruments as mentioned in the preceding part describing spectra of component A.

- 38 spectra obtained using the Ondřejov coudé spectrograph between 17 October 2003 and 22 March 2008.
- One *HEROS* spectrum obtained at the Ondřejov Observatory, one night after the HR 1847A spectrum, on 23 March 2003.
- Three spectra between 28 August 2007 and 30 August 2007 obtained at the Rozhen Observatory.

3.1. Radial velocity measurements

Radial velocities were measured using the code SPEFO, which was developed by the late Dr. Jiří Horn (see also Škoda, 1996). The FITS files obtained from IRAF and MIDAS were transformed to the SPEFO format, and then the radial velocities (RVs) were obtained interactively by means of the best match of the line profile with its mirror. The RVs were obtained for hydrogen $H\alpha$, He I 6678 Å, Si II 6347 Å and 6371 Å lines. RV data for individual components are described later in this paper in Sections 4.2 and 5.1.

4. Component A

4.1. The effective temperature and gravity

The spectral region observed by *HEROS* covered the range 3800–8620 Å (see Figs. A.1 and A.2) and was used to determine the spectroscopic effective temperature and surface gravity. The line spectrum of the star is quite poor. Balmer lines up to H10 and some infrared lines are seen. No emission is present in the Balmer lines and in the lines of other metal ions.

The effective temperature and surface gravity were determined by comparing the observed spectra to model spectra.

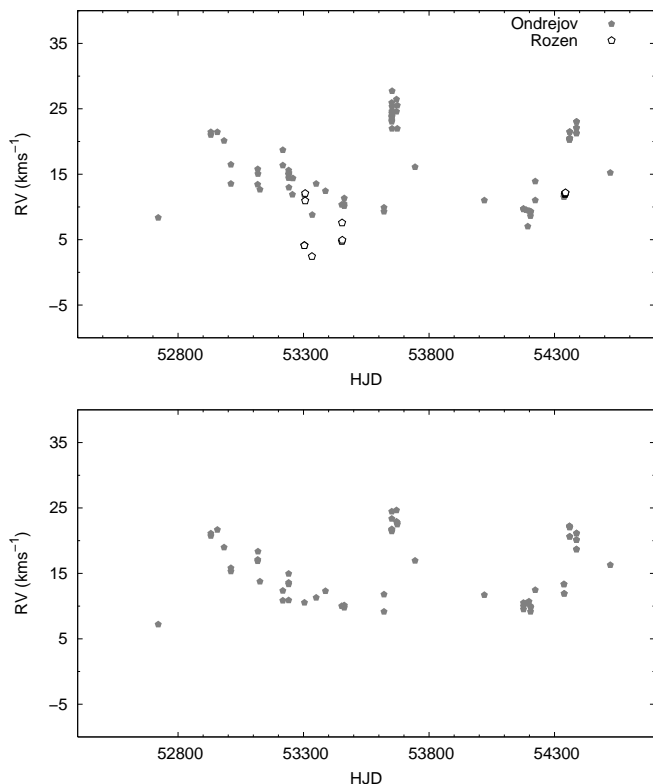


Fig. 1. The radial velocity variations for hydrogen $H\alpha$ (upper panel) and $\text{He I } 6678 \text{ \AA}$ (lower panel) lines measured from the Ondřejov and Rozhen spectrograms as a function of HJD. The $\text{He I } 6678 \text{ \AA}$ line is only present in the Ondřejov spectra. Full symbols represent Ondřejov data, and open symbols stand for Rozhen data. All values are from Tables A.1 and A.2.

We used the ATLAS9 LTE line blanketed model atmospheres, which were calculated by Kurucz (1993) assuming solar metallicity and microturbulent velocity 2 km s^{-1} . All synthetic spectra were convolved (using the code ROTIN3 by I. Hubeny) with the Gaussian function having $\text{FWHM}=0.25$ to reduce the resolution of the synthetic spectra to the observed resolution. We used a χ^2 -fitting routine to compare the whole observed spectra with the synthetic ones, and we obtained a best fit of $T_{\text{eff}} = (12500 \pm 500) \text{ K}$ and $\log g = 3.5 \pm 0.5$. Following the temperature scale of Theodosiou & Danezis (1991), these values correspond to spectral type B7 – B8, and from the value of the surface gravity, we estimate the luminosity class as IV – V. The quoted error bars correspond to the adopted steps of our model grid, which are 500 K in temperature and 0.5 in $\log g$.

Using the code ROTIN3, we calculated a grid of rotationally broadened spectra for $5 \text{ km s}^{-1} \leq v \sin i \leq 500 \text{ km s}^{-1}$ with a step of 5 km s^{-1} . Then we applied the χ^2 fitting routine again to determine the best rotational velocity for this star. To do this, we used the spectral line $\text{Mg II } 4481 \text{ \AA}$ (recommended by Gray, 1976, as a line free of pressure broadening) in the fitting process. We determined the projected rotational velocity of HR 1847A as $v \sin i = (40 \pm 3) \text{ km s}^{-1}$, which differs by 5 km s^{-1} from the value of Abt et al. (2002). The error of our value of the rotational velocity was calculated employing a $1-\sigma$ error algorithm of Zhang et al. (1986).

4.2. Radial velocities

Tables A.1 and A.2 display the line radial velocity measurements that were derived using the methods described in Section 3.1. Columns 1, 2, and 3 represent the file identification, HJD, and the heliocentric RVs, respectively. Column 4 lists the RV measurements for the $H\alpha$ line. Columns 5, 6, and 7 list the RVs measurements for $\text{He I } 6678 \text{ \AA}$, $\text{Si II } 6347 \text{ \AA}$, and $\text{Si II } 6371 \text{ \AA}$ (which are weak) absorption lines, respectively. The measured RVs were shifted to the zero-point using a set of sharp telluric absorption lines by means of the technique described in Horn et al. (1996).

The RVs of HR 1847A vary between 8 km s^{-1} to 27 km s^{-1} with a mean velocity around 13 km s^{-1} . Figure 1 displays the measured RVs for hydrogen $H\alpha$ and $\text{He I } 6678 \text{ \AA}$ as a function of time. The plots indicate that our RV measurement started with one value just before the RV maximum, then after the maximum, a clear decrease in the RV values is recorded until the RV values reach their minimum around HJD 2453620 with RV values of $9\text{--}10 \text{ km s}^{-1}$. Then they quickly reached the next maximum value of 27 km s^{-1} around HJD 2453670. Although only two cycles are covered by our observations, fortunately we successfully recorded two epochs of rapid rise to the maximum, which happened during a very short time (nearly 35 days) of the long cycle. Rozhen observations confirmed the present distribution of RVs. Such a relatively short event could easily be missed.

The RV measurements that were obtained with different lines in the $H\alpha$ region show the same distribution with time, and only a small difference in the maximum height can be recognized, as illustrated for the $\text{He I } 6678 \text{ \AA}$ line (lower panel of Fig. 1).

4.3. Period determination

One of the most fundamental parameters of binary systems is the orbital period. The present RVs span an interval of 1801 days. From the inspection of the time plot one can conclude that

1. the present RV measurements of $H\alpha$ and of some other metallic lines show clear evidence of long-term cyclic variability, and
2. the relatively large scatter between individual measurements on successive nights indicates that shorter period variability could be present in the data distribution.

No period search of the RV measurements has been carried out so far for HR 1847A. Improper data distribution, gaps, and timing of the observations are the most common problems in the period search process. The period search was carried out separately for several sets of measurements, and two independent numerical period searching routines were used. The first one is based on the phase dispersion minimization (PDM) technique (Stellingwerf, 1978), the other one, PERIOD (Breger, 1990), is based on a Fourier analysis.

For PERIOD, starting values for the frequencies need to be given, and frequency values are improved within the limits given by the window function. We used this program to search for periodicities in both $H\alpha$ and $\text{He I } 6678 \text{ \AA}$ RV data sets in the

Table 2. Candidate frequencies resulting from the PDM period search.

frequency (d^{-1})	period (days)	θ
0.0069	144.92753	0.3841
0.0014	714.28571	0.4092
0.1077	9.28505	0.4668

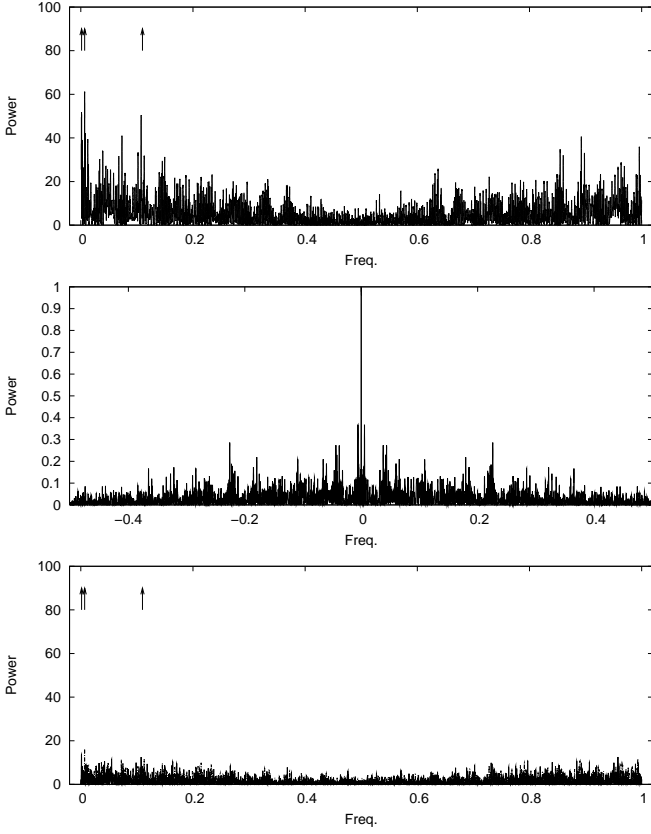


Fig. 2. *Upper panel:* Power spectrum of measured RVs of $H\alpha$ and $He\ I\ 6678\ \text{\AA}$ in the frequency range from $0.001\ \text{d}^{-1}$ to $1\ \text{d}^{-1}$, *middle panel:* spectral window, and *lower panel:* power spectrum of the prewhitened residual with $0.0014\ \text{d}^{-1}$. In all panels frequencies at the x -axis are given in d^{-1} .

range between 1 to 1000 days, with an expected frequency resolution of $0.00055\ \text{d}^{-1}$. The upper panel of Fig. 2 displays the periodogram of the detected frequencies in this period range. It shows three candidate frequencies (indicated by arrows in the upper panel of Fig. 2), namely $0.0069\ \text{d}^{-1}$, $0.0014\ \text{d}^{-1}$, and $0.1077\ \text{d}^{-1}$. The frequency $0.0069\ \text{d}^{-1}$ has power 61, and is dominant. The middle panel of Fig. 2 shows the spectral window. In the lower panel of Fig. 2 we show the power spectrum of the residual periodogram prewhitened for $0.0014\ \text{d}^{-1}$ (using PERIOD), which clearly shows the disappearance of all peaks related to all three candidate frequencies.

Using the PDM technique we searched for periodicity in intervals 1–10 days, 1–100 days, and 1–1000 days. The results are summarized in Table 2 and agree with the ones obtained with PERIOD. Figure 3 illustrates the phase diagrams of measured RVs for the $H\alpha$ line folded with the $0.1077\ \text{d}^{-1}$, $0.0069\ \text{d}^{-1}$ and $0.0014\ \text{d}^{-1}$ frequencies.

Although the frequency $0.0069\ \text{d}^{-1}$ has the highest power (cf. Fig. 2 and Table 2), we suspect that this frequency is not a real one. First, the historical observations of Plaskett & Young (1919) are out of phase by about half of the period (open squares in the middle panel of Fig. 3). Second, the corresponding RV curve predicts a maximum of RVs near HJD 2453350, which was not confirmed by our observations. Values around $\sim 15\ \text{km s}^{-1}$ appear instead of maximum ones. In addition, the interval of 145 days (or approximately five months) roughly corresponds to the gap between the end of one season in March/April and the next start of observations in August/September. Third,

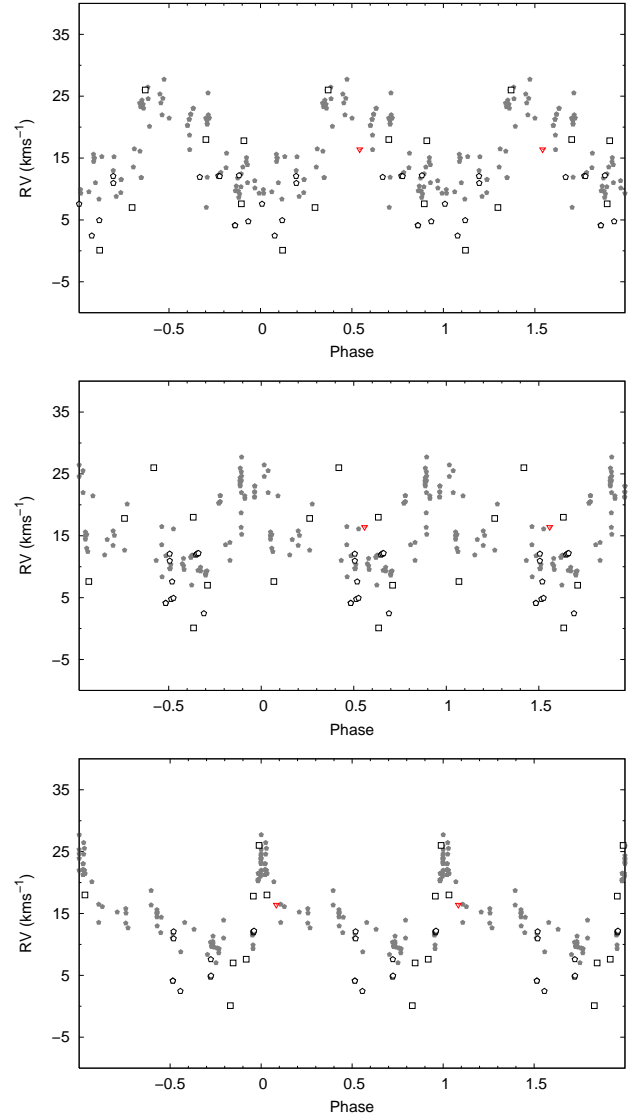


Fig. 3. Phase diagram of measured RVs for $H\alpha$ lines folded with different frequencies displayed from top to bottom, $0.1077\ \text{d}^{-1}$ ($9^{\text{d}}28505$), $0.00689\ \text{d}^{-1}$ ($144^{\text{d}}9275$), and $0.0014\ \text{d}^{-1}$ ($714^{\text{d}}2857$). Filled circles (●) and open circles (○) denote data obtained from our observations at Ondřejov and Rozhen, respectively. Open squares (□) and open triangles (▽) represent data from Plaskett & Young (1919) and Vieira et al. (2004), respectively.

the candidate frequency $0.0069\ \text{d}^{-1}$ is almost exactly equal to $5 \times 0.0014\ \text{d}^{-1}$. The relative scatter of individual RV values folded with the $0.1077\ \text{d}^{-1}$ frequency is quite large. Following these arguments, we propose the frequency at $0.0014\ \text{d}^{-1}$ as the dominant frequency.

4.4. Orbital solution

The variability of the radial velocities with frequency $0.0014\ \text{d}^{-1}$ can most likely be explained by binarity, and it supports the earlier idea of Plaskett & Young (1919) that the star is a spectroscopic binary.

Starting from the frequency $0.0014\ \text{d}^{-1}$, we performed 4 different orbital solutions using the program FOTEL developed by Hadrava (1990, 2004). For the solutions denoted as I, II, and III (see Table 3), the orbital elements were derived for $H\alpha$ ra-

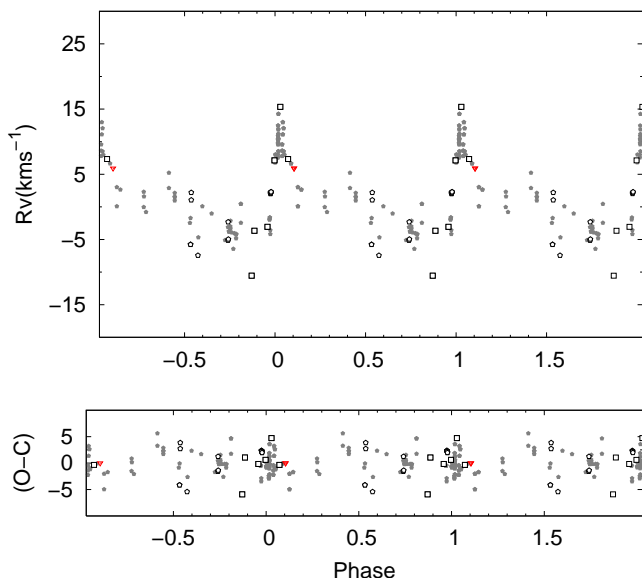


Fig. 4. *Upper panel:* Radial velocity curve of the primary component corresponding to the FOTEL orbital solution III ($P = 719^d.79$), which was based on $H\alpha$ RV measurements of Ondřejov, Rozhen, and OPD spectra and on RV values from Plaskett & Young (1919). RV values are displayed in the centre-of-mass reference system. *Lower panel:* Phase plot of $O - C$ deviation from the RV curve for Solution III.

dial velocity variations with data observed from different sites. Solution I is only performed with Ondřejov data, Solution II is obtained using $H\alpha$ measurements from both Ondřejov and Rozhen observations, Solution III is obtained using all of the available data, namely Ondřejov and Rozhen observations, one spectrum from OPD, and including the historical measurements. Solution IV was obtained using radial velocities of all available spectral lines in the $H\alpha$ region ($H\alpha$, He I 6678 Å, Si II 6347 Å, and Si II 6371 Å).

In our calculations we allowed the period, eccentricity, periastron longitude, and semiamplitude to converge. For each data set FOTEL also allows individual γ -velocities to be determined. Figure 4 illustrates the FOTEL Solution III with its $O - C$ residuals. We searched for additional periodicities in the residuals but did not find any significant periods.

We adopt the Solution III ($P = 719^d.79 \pm 0^d.17$, $e = 0.70 \pm 0.02$) as an orbital solution of HR 1847A.

5. Component B

The B component is a Be star with a relatively weak emission in $H\alpha$ and almost negligible one in $H\beta$. Since 2003, the weak emission in $H\alpha$ further weakened, indicating an approaching end of the Be phase. No time scale may be given for this apparently long-term variability, since only 4 years of observations are available. Long term variability (strengthening and weakening of emission) is typical of Be stars on time scales from years to tens of years (for a review see Hubert, 2007). For example, α Dra has quite a well-established long term time scale, and its most recent determination is 22.11 years (see Kubát et al., 2010, and references therein). The $H\alpha$ profiles obtained by our observations are plotted in Figure 5. We fitted the spectrum of component B using the same methods as for component A.

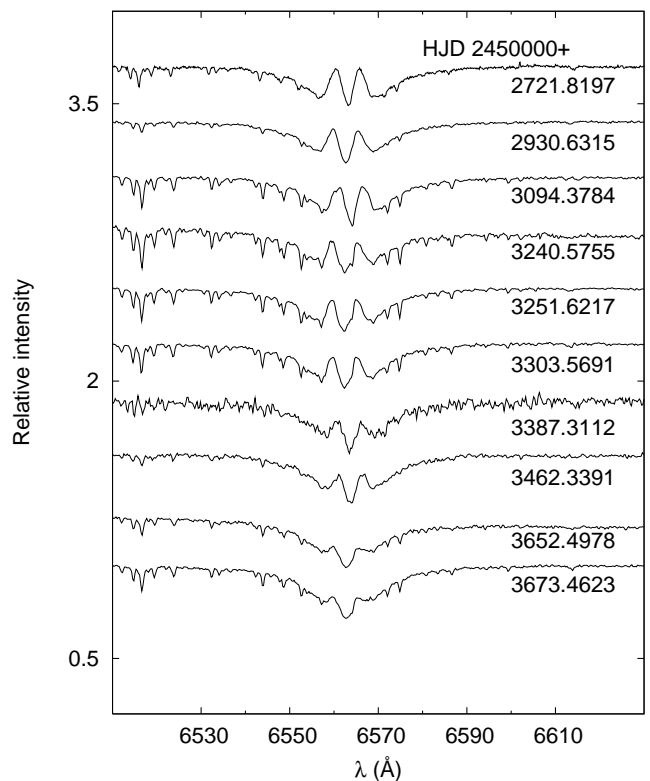


Fig. 5. The evolution of the $H\alpha$ profile of HR 1847B.

We found $T_{\text{eff}} = (12500 \pm 500)$ K, $\log g = (3.5 \pm 0.5)$, and $v \sin i = (230 \pm 5)$ km s $^{-1}$.

5.1. Radial velocities

Owing to the high rotational broadening of lines in the component B spectrum, the helium and silicon lines, which were used for RV measurement of component A, are too shallow in component B, and therefore unusable for RV measurement. Consequently, we measured the RVs of component B only from the $H\alpha$ line. RVs were measured with the profile inversion technique. However, the rapid rotation of the component B and rela-

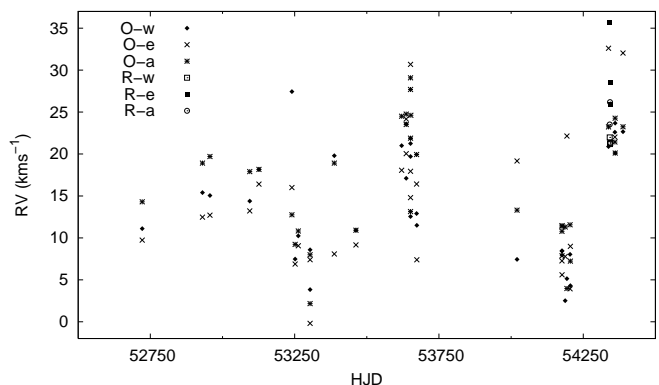


Fig. 6. Time evolution of the $H\alpha$ radial velocities of HR 1847B. Measurements of line wings are denoted by w, measurements of emission are denoted by e, and measurement of the central absorption are denoted by a. Capital letters denote the observatory, R stands for Rozhen, O stands for Ondřejov.

tively low S/N made it impossible to arrive at precise RV values. Cross-correlation techniques, such as least-square deconvolution (LSD, Donati et al., 1997) would not improve the RV accuracy as too few line profiles are available in our spectra. Also, the bisector method does not give more accurate results because of the limited quality and not high enough S/N of our spectra.

The H α line in the B component is characterized by a double-peak emission with peaks of equal strength. We measured the RVs of three different features at the H α line, namely of the line wings, of the emission part, and of the central absorption. The results are listed in Tables A.3 and A.4 and plotted in Fig. 6.

Although the RVs are evidently variable, a period search did not give any reasonable result. That is why we cannot make any conclusions about the possible binarity of HR 1847B until a more complete set of more accurate data has been obtained.

6. The possible A+B system

There is a question as to whether the components of this visual pair are physically bound. However, there is not enough data to help to resolve this question. The history of all relative position measurements of HR 1847 in the sky (see Section 2.1.1) do not allow any conclusion about their relative motion. Slightly different values can be attributed to errors in individual measurements.

Unfortunately, only a common parallax measurement from HIPPARCOS is available. Since individual measurements are missing, we cannot easily say whether the A and B components are at the same distance. However, study of visual binaries by Shatskii (1998) suggests that HR 1847 could be a physical system (with a period shorter than 1 Myr), since both components have similar proper motion and corresponding photometric parallaxes, which agree with the hypothetical parallax.

In case the visual components of HR 1847 are physically bound, their similar spectral type suggests that they are of similar age. Then there is the question of why one of these stars developed an envelope that causes H α emission and the other does not. The emission could not be caused by mutual interaction between components A and B, simply because the distance between the components is too large. A different mechanism for the origin of the Be phenomenon in HR 1847B has to be found (see, e.g., the review by Porter & Rivinius, 2003). The emission in the component B is most probably connected with its rapid rotation. Projected rotational velocity of component A is lower, and this star also has no emission. On the other hand, since the inclination angles are unknown, we can not exclude the possibility that the component A is also rapidly rotating, as there is apparently no correlation between directions of spin axes for wide binaries (Howe & Clarke, 2009).

6.1. Comparison with other visual binaries

HR 1847 is not the only example of a visual multiple system with similar components, with some of them also showing the Be phenomenon. The visual triple system β Mon consists of three Be stars (see Marañón di Leo et al., 1994, and references therein), and all these three stars are rapidly rotating (Abt et al., 2002). The projected rotational velocities of β Mon A and β Mon C was reported as 260 km s⁻¹ and 250 km s⁻¹, respectively, while β Mon B is rotating more slowly (140 km s⁻¹) and, interestingly, also has weakest emission (Cowley & Gugula, 1973). This supports the connection between rapid rotation and the Be phenomenon. More visual binaries with Be-components may be found in Abt & Cardona (1984).

Table 4. Summary of parameters of both components of HR 1847.

	HR 1847A	HR 1847B
α (J2000)	05 32 14.14	05 32 14.56
δ (J2000)	+17 03 29.3	+17 03 21.8
V	6.09	6.51
T_{eff}	12500 \pm 500	12500 \pm 500
$\log g$	3.5 \pm 0.5	3.5 \pm 0.5
$v \sin i$ (km s ⁻¹)	40 \pm 3	230 \pm 5
Be star	no	yes
binary	SB1*	SB1?

* – Binary parameters are listed in Table 3

Investigation of such multiple systems with resolved visual components (like HR 1847 or β Mon) may help when studying multiple partially resolved or unresolved systems with Be stars like α And (see Olević & Cvetković, 2006, and references therein) or β Cep (see Wheelwright et al., 2009, and references therein), where light from all stars is mixed, making the analysis extremely difficult. The physical parameters and system characteristics derived from resolved systems will put constraints on stellar structure and binary evolution models, such that the unresolved systems can be modelled in a better way with the improved models. Careful study of resolved systems and careful determination of their parameters are very important feedback on models.

7. Conclusions

This paper is the first attempt to collect all available information about the stars in the visual binary system HR 1847 and to correct errors that appear in the SIMBAD database and Bright Star Catalogue. We have presented results of our spectroscopic analysis. HR 1847A ($V = 6.09$, Shatskii, 1998) is a B type single-lined, eccentric, ($e = 0.70 \pm 0.02$), spectroscopic binary with a period of 719.79 ± 0.17 days. Model atmosphere analysis of this star yielded $T_{\text{eff}} = 12500$ K, $\log g = 3.5$, and $(v \sin i)_A = 40$ km s⁻¹. HR 1847B ($V = 6.51$, Shatskii, 1998) is a Be star with variable radial velocities, however, no reasonable orbital solution could be found based on the available data. Model atmosphere analysis of this star yielded the same effective temperature and surface gravity as for the A component, but with a rotational velocity of $(v \sin i)_B = 230$ km s⁻¹. A decrease in the H α emission was recorded during the last 4.5 years of observations. In addition, positions of X-ray (1RXS J053214.9+170319, see Section 2.8) and infrared (X0501+589, see Section 2.9) sources indicate that HR 1847B is more likely an X-ray and IR source than HR 1847A.

Several other issues, such as the short term variability of HR 1847A or the reliable period determination of HR 1847B, could not be addressed by this paper owing to the lack of necessary data. Consequently, further long-term observations of these stars are desirable. Future work should also include a detailed abundance analysis using high S/N spectra and NLTE model atmospheres.

Acknowledgements. The authors would like to devote this paper to the memory of Dr. Izold Pustynnik, with whom they consulted for the history of Struve's observations in Tartu. The authors would also like to thank Zdeněk Janák, Jan Elner, and Petr Švaříček for their help in early stages of the work. This research made use of the Washington Double Star Catalog maintained at the U.S. Naval Observatory. This research has made use of the NASA's Astrophysics Data System Abstract Service. Our work was supported by a grant of the Grant Agency of the Czech Republic 205/08/0003. The Astronomical Institute Ondřejov is supported by project AV0 Z10030501.

References

- Abbott, D. C. 1980, *ApJ* 242, 1183
- Abt, H. A., & Cardona, O. 1984, *ApJ* 285, 190
- Abt, H. A., Levato, H., & Grosso, M. 2002, *ApJ* 573, 359
- Andrews, P. J. 1968, *MemRAS* 72, 35
- Breger, M. 1990, *A&A* 240, 308
- Berghöfer, T. W., Schmitt, J. H. M. M., & Cassinelli, J. P. 1996, *A&AS* 118, 481
- Berghöfer, T. W., Schmitt, J. H. M. M., Danner, R., & Cassinelli, J. P. 1997, *A&A* 322, 167
- Cannon, A. J. 1912a, *Ann. Harvard College Observatory* 56, 65
- Cannon, A. J. 1912b, *Ann. Harvard College Observatory* 56, 227
- Cannon, A. J., & Pickering, E. C. 1918, *Ann. Harvard College Observatory* 92, 1
- Coté, J., Waters, L. B. F. M. 1987, *A&A* 176, 93
- Cowley, A., & Gugula, E. 1973, *A&A* 22, 203
- Cowley, A., Cowley, C., Jaschek, M., & Jaschek, C. 1969, *AJ* 74, 375
- Donati, J.-F., Semel, M., Carter, B. D., Rees, D. E., & Collier Cameron, A. 1997, *MNRAS*, 291, 658
- Duflot, M., Fehrenbach, C., Mannone, C., Burnage, R., & Genty, V. 1992, *A&AS* 110, 177
- Eggen, O. J. 1977, *PASP* 89, 205
- Fabricius, C., Høg, E., Makarov, V. V., et al. 2002, *A&A* 384, 180
- Flesch, E., & Hardcastle, M. J. 2004, *A&A* 427, 387
- Frost, E. B., Barrett, S. B., & Struve, O. 1926, *ApJ* 64, 1
- Gahm, G. F., Ahlin, P., & Lindroos, K. P. 1983, *A&AS* 51, 143
- Gray, D. F. 1976, *The observation and analysis of stellar photospheres*, John Wiley & Sons, New York
- Hadrava, P. 1990, *Contrib. Astron. Obs. Skalnaté Pleso* 20, 23
- Hadrava, P. 2004, *Publ. Astron. Inst. ASCR* 92, 1
- Herschel, W. 1785, *Phil. Trans. Roy. Soc. London* 75, 40
- Herschel, W. 1821, *Mem. Astron. Soc.* 1, 166
- Hoffleit D., & Jaschek, C. 1991, *The Bright Star Catalogue*, 5th Revised Ed., Yale University Observatory, New Haven
- Horn, J., Kubát, J., Harmanec, P., et al. 1996, *A&A* 309, 521
- Howe, K. S., & Clarke, C. J. 2009, *MNRAS* 392, 448
- Hubert, A.-M. 2007, in *Active OB-Stars: Laboratories for Stellar & Circumstellar Physics*, S. Štefl, S. P. Owocki, & A. T. Okazaki eds., *ASP Conf. Ser. Vol. 361*, p. 27
- Iwata, I., Okumura, S., & Saitō, M. 1999, *PASJ* 51, 653
- Kaufer, A. 1998, *Rev. Mod. Astron.* 11, 177
- Kharchenko, N. V. 2001, *Kin. Fiz. Neb. Tel* 17, 409
- Kharchenko, N. V., Piskunov, A. E., Roeser, S., Schilbach, E., & Scholz, R.-D. 2004, *AN* 325, 740
- Kubát, J., Saad, S. M., Šlechta, M., Yang, S. 2010, in *Binaries – Key to Comprehension of the Universe*, A. Prša & M. Zejda eds., *ASP Conf. Ser.*, in press
- Kurucz, R. L. 1993, *ATLAS9 Stellar Atmosphere Programs and 2 km/s grid*, Kurucz CD-ROM No.13
- Levato, H., 1975, *A&A* 19, 91
- Lindroos, K. P. 1983, *A&AS* 51, 161
- Magnier, E. A., Volp, A. W., Laan, K., van den Ancker, M. E., & Waters, L. B. F. M. 1999, *A&A* 352, 228
- Marañón di Leo, C., Colombo, E., & Ringuelet, A. E. 1994, *A&A* 286, 160
- Mason, B. D., Hartkopf, W. I., Wycoff, G. L., et al. 2004, *AJ* 127, 539
- Mora, A., Merín, B., Solano, E., et al. 2001, *A&A* 378, 116
- Olević, D., & Cvetković, Z. 2006, *AJ* 131, 1721
- Osawa, K. 1959, *ApJ* 130, 159
- Oudmajer, R. D., Palacios, J., Eiroa, C., et al. 2001, *A&A* 379, 564
- Percy, J. R., Harlow, C. D. W., & Wu, A. P. S. 2004, *PASP* 116, 178
- Perryman, M. A. C., & ESA 1997, *The Hipparcos and Tycho catalogues*, ESA SP Ser. Vol. 1200, ESA, Noordwijk
- Plaskett, J. S. 1919, *JRASC* 13, 197
- Plaskett, J. S., Young, R. K. 1919, *JRASC* 13, 191
- Plaskett, J. S., Harper, W. E., Young, R. K., & Plaskett, H. H. 1920, *Publ. Dominion Astrophys. Obs.* 1, 163
- Porter, J. M., & Rivinius, Th. 2003, *PASP* 115, 1153
- Russell, H. N., & Moore, C. E. 1929, *AJ* 39, 165
- Shatskii, N. I. 1998, *PAZh* 24, 307 (*Astron. Lett.* 24, 257)
- Škoda, P. 1996, in *Astronomical Data Analysis Software and Systems V*, G. H. Jacoby & J. Barnes eds., *ASP Conf. Ser. Vol. 101*, p. 187.
- Škoda, P., & Šlechta, M. 2002, *Publ. Astron. Inst. ASCR* 90, 40
- Skrutskie, M. F., Cutri, R. M., Stiening, R., et al. 2006, *AJ* 131, 1163.
- Slettebak, A. 1963, *ApJ* 138, 118
- Stahl, O., Kaufer, A., Wolf, B. et al. 1995, *J. Astron. Data* 1, 3
- Stellingwerf, R. F. 1978, *ApJ* 224, 953
- Struve, F. G. W. 1837, *Stellarum Duplicium et Multiplicium Mensurae Micrometricae*, Ex Typographia Academica, Petropoli
- Theodossiou, E., & Danezis E., 1991, *Ap&SS* 183, 91
- van Leeuwen, F. 2007, *A&A* 474, 653
- Vieiria, S. L. A., Corradi, W. J. B., Alencar, S. H. P., et al. 2003, *AJ* 126, 2971
- Voges, W., Aschenbach, B., Boller, Th. 2000, *IAUC* 7432, 15944
- Wackerling, L. R. 1970, *PASP* 82, 1357
- Wheelwright, H. E., Oudmajer, R. D., & Schnerr, R. S. 2009, *MNRAS* 497, 487
- Whitelock, P. A., Feast, M. W., & Catchpole, R. M. 1989, *MNRAS* 238, 7p
- Zhang, E.-H., Robinson, E. L., & Nather, R. E., 1986, *ApJ* 305, 740

Table 3. Orbital elements of HR 1847A with FOTEL.

Element	Solution I	Solution II	Solution III	Solution IV
P[d]	715.03 ± 1.06	713.83 ± 1.49	719.79 ± 0.17	710.49 ± 0.98
$T_{\text{periastr.}}$	51501.61 ± 4.26	51504.34 ± 5.93	51480.31 ± 3.88	51503.67 ± 3.09
K (km s ⁻¹)	7.89 ± 0.53	7.58 ± 0.55	7.73 ± 0.44	8.23 ± 0.23
e	0.79 ± 0.02	0.72 ± 0.03	0.70 ± 0.02	0.73 ± 0.01
ω [deg]	306 ± 5.87	310 ± 6.99	304 ± 7.03	286 ± 3.70
γ_1 (km s ⁻¹)	13.47	13.39	13.44	–
γ_2 (km s ⁻¹)	–	9.54	9.88	–
γ_3 (km s ⁻¹)	–	–	10.63	–
γ_4 (km s ⁻¹)	–	–	10.52	–
γ_5 (km s ⁻¹)	–	–	–	13.23
γ_6 (km s ⁻¹)	–	–	–	13.36
γ_7 (km s ⁻¹)	–	–	–	10.97
γ_8 (km s ⁻¹)	–	–	–	13.10
$f(m)$	0.0095	0.0104	0.0126	0.0132
No. of RVs	64	76	83	246
rms (km s ⁻¹)	1.76	2.08	2.22	1.94

Note: The velocity γ_1 is based on Ondřejov data, γ_2 on Rozhen data, γ_3 on OPD data (Vieiria et al., 2004), and γ_4 on historical data of Plaskett & Young (1919). In solution IV γ_5 , γ_6 , γ_7 , and γ_8 stand for H α , He I 6678 Å, Si II 6347 Å, and Si II 6371 Å, respectively.

Appendix A: Visual spectra of HR 1847A and HR 1847B.

Table A.2. Heliocentric radial velocities (RV) of HR 1847A – spectra from Rozhen Observatory.

file	HJD (JD–2400000)	V_{hel} (km s^{-1})	$RV(\text{H}\alpha)$ (km s^{-1})
04j119	53303.4455	23.17	10.52
04j120	53303.4563	23.16	9.14
04j303	53306.5530	21.99	11.16
04j304	53306.5638	21.97	12.06
04k109	53333.3218	10.99	8.39
05c062	53452.6889	–29.64	4.76
05c163	53453.3861	–29.56	7.58
05c235	53454.4102	–29.47	4.93
07h050	54341.5910	28.25	11.92
07h129	54342.5379	28.43	12.12
07h135	54342.6011	28.36	12.05
07h215	54343.5844	28.52	12.19

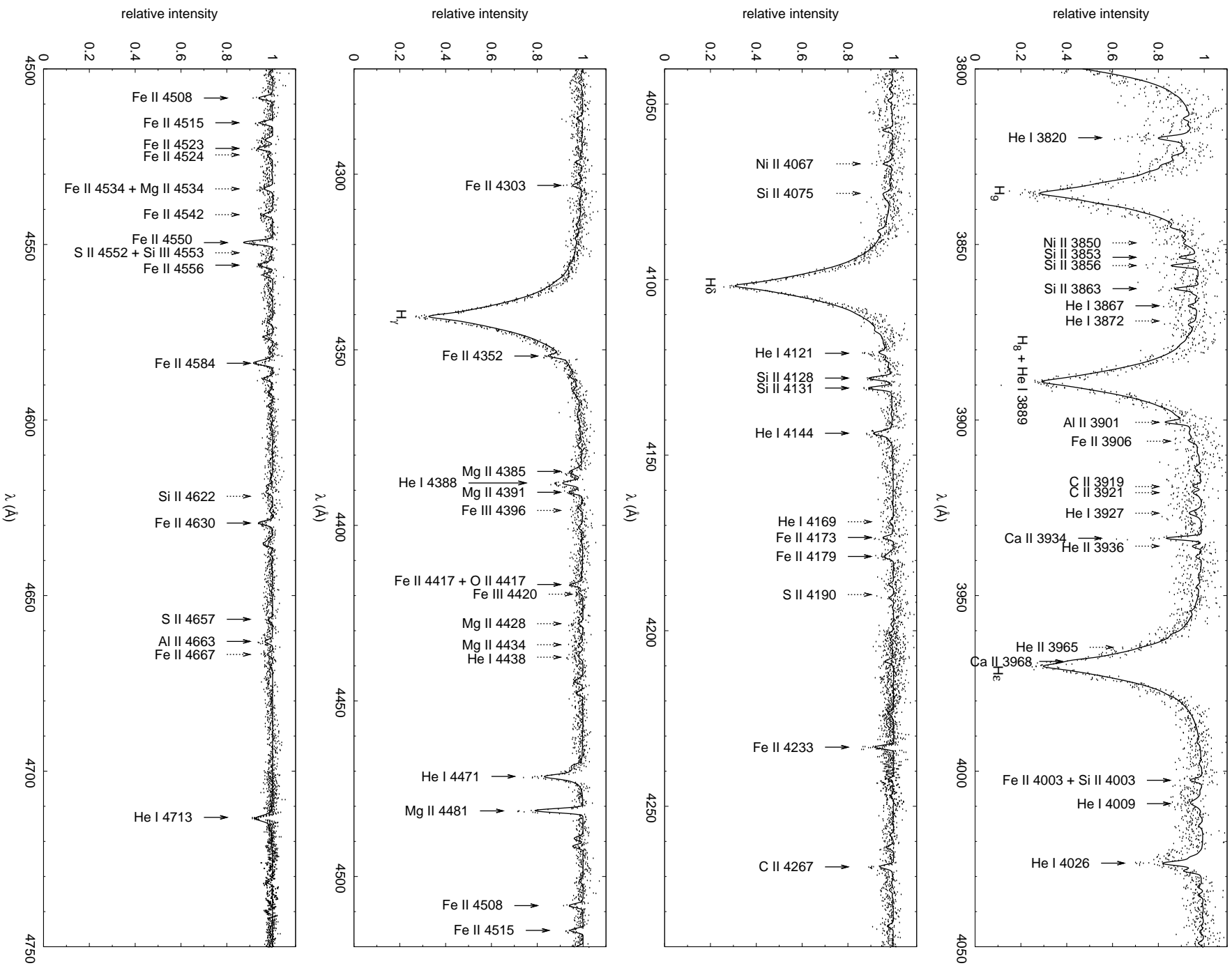


Fig. A.1. Line identification of the spectrum of HR 1847 A obtained with the blue channel of the HEROS spectrograph (dots) and comparison with the synthetic spectrum calculated from the Kurucz (1993) LTE model atmosphere $T_{\text{eff}} = 12500$ K, $\log g = 3.5$, rotationally broadened with $(v \sin i)_{\lambda} = 40$ km s $^{-1}$ (full line).

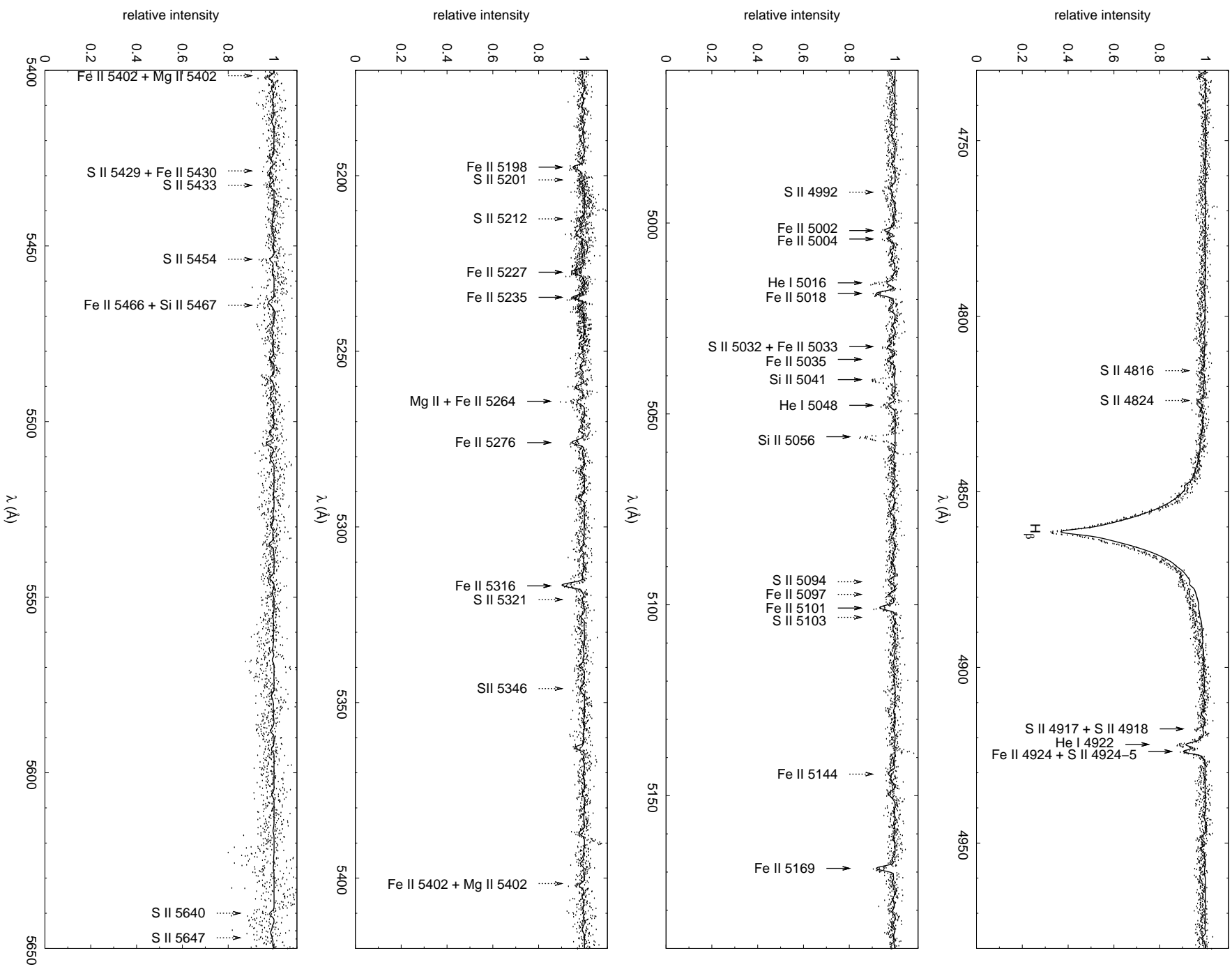


Fig. A.1. contd.

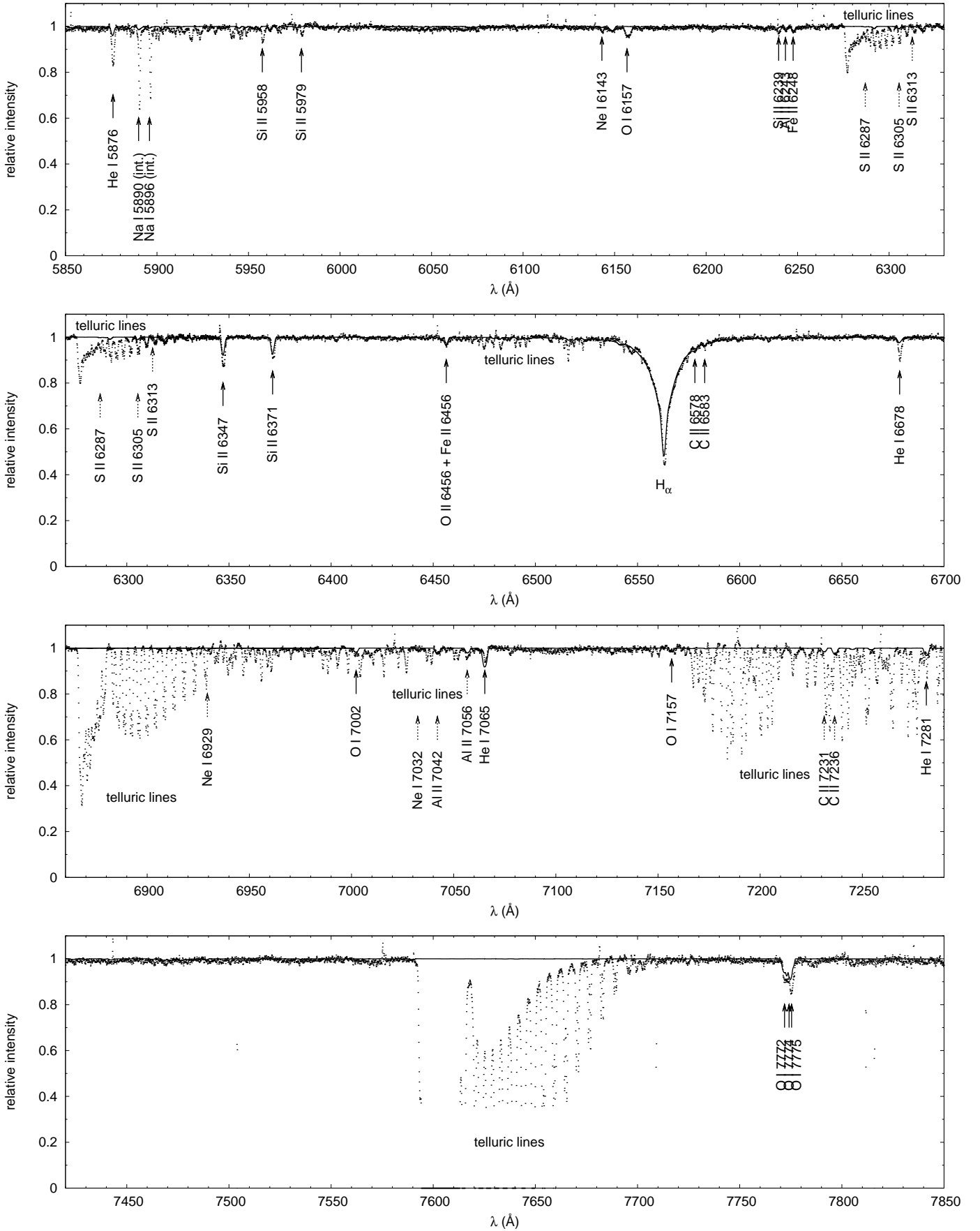


Fig. A.2. Line identification of the spectrum of HR 1847A obtained with the red channel of the *HEROS* spectrograph (dots) and comparison with the synthetic spectrum calculated from the Kurucz (1993) LTE model atmosphere $T_{\text{eff}} = 12\,500\text{ K}$, $\log g = 3.5$, rotationally broadened with $(v \sin i)_A = 40\text{ km s}^{-1}$ (full line). Note the presence of telluric lines and bands near 6280 \AA , $H\alpha$, 6870 \AA , 7250 \AA , and 7590 \AA .

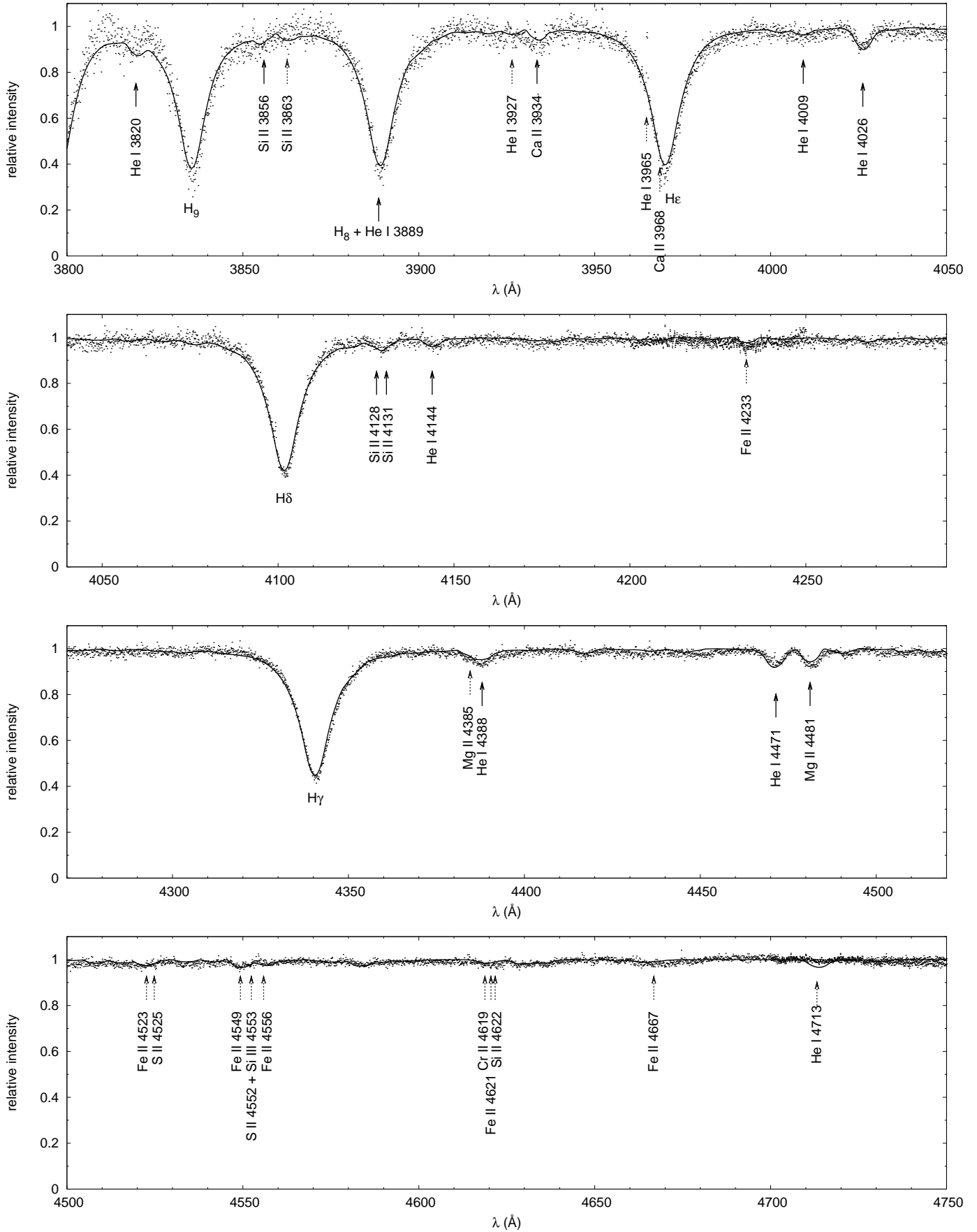


Fig. A.3. Line identification of the spectrum of HR 1847B obtained with the blue channel of the *HEROS* spectrograph (dots) and comparison with a synthetic spectrum calculated from the Kurucz (1993) LTE model atmosphere $T_{\text{eff}} = 12\,500\text{ K}$, $\log g = 3.5$, rotationally broadened with $(v \sin i)_B = 230\text{ km s}^{-1}$ (full line).

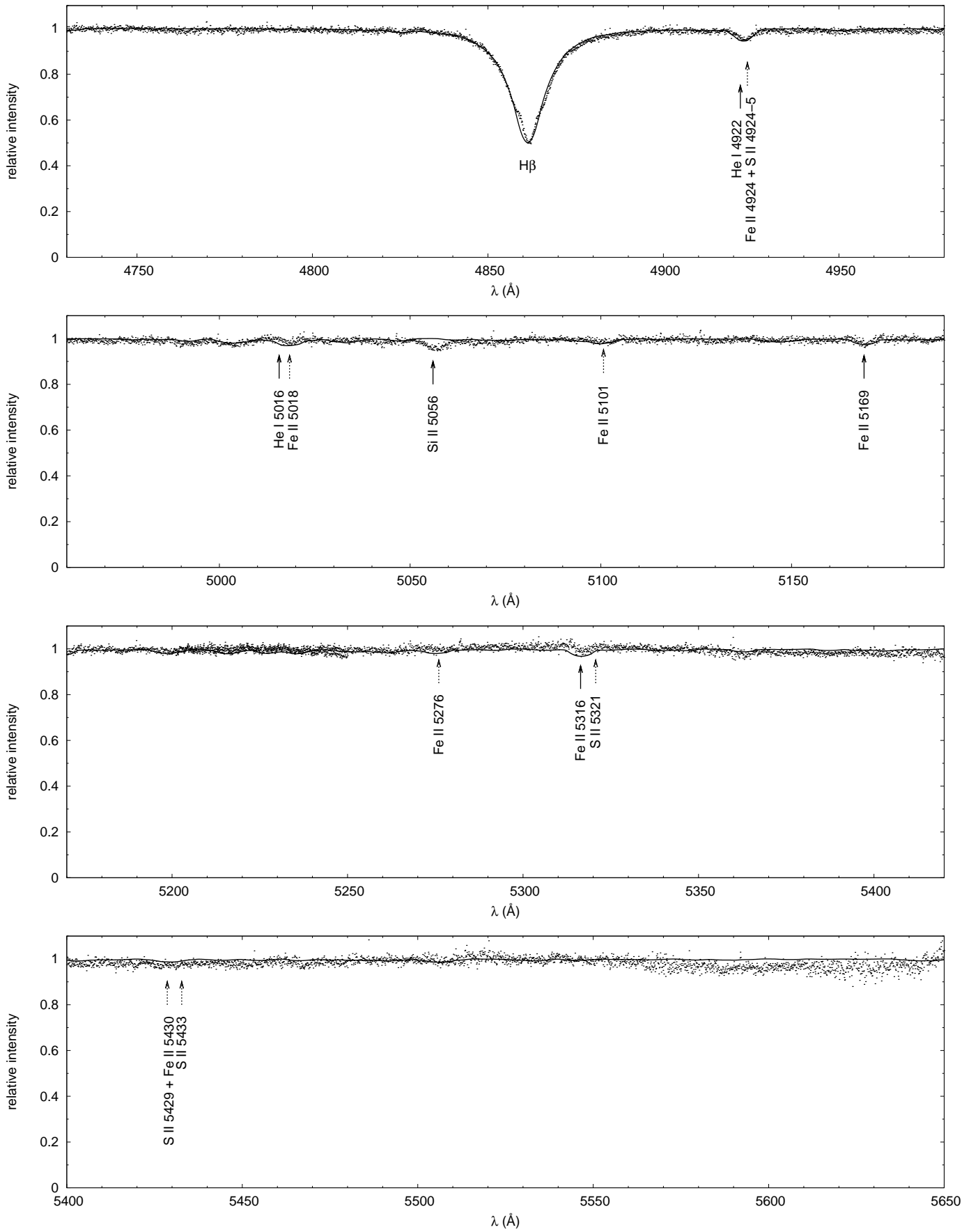


Fig. A.3. contd.

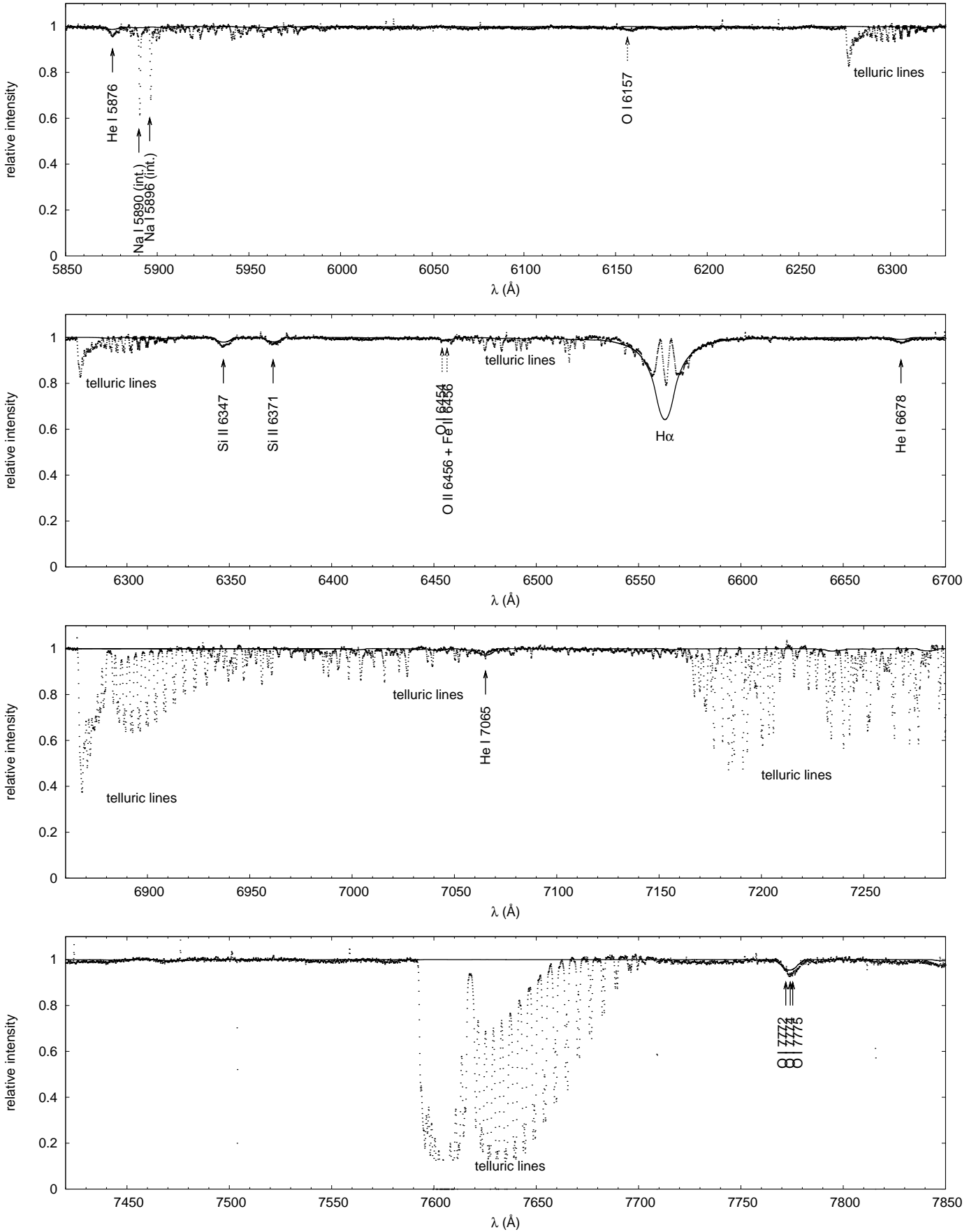


Fig. A.4. Line identification of the spectrum of HR 1847B obtained with the red channel of the *HEROS* spectrograph (dots), and comparison with a synthetic spectrum calculated from the Kurucz (1993) LTE model atmosphere $T_{\text{eff}} = 12\,500\text{ K}$, $\log g = 3.5$, rotationally broadened with $(v \sin i)_B = 230\text{ km s}^{-1}$ (full line). Note the presence of telluric lines and bands near 6280 \AA , $H\alpha$, 6870 \AA , 7250 \AA , and 7590 \AA .

Table A.1. Heliocentric radial velocities (RV) of HR 1847A – spectra from Ondřejov Observatory, where V_{hel} is the heliocentric velocity.

file	HJD (JD–2400000)	V_{hel} (km s^{-1})	$RV(\text{H}\alpha)$ (km s^{-1})	$RV(\text{He I } 6678 \text{ \AA})$ (km s^{-1})	$RV(\text{Si II } 6347 \text{ \AA})$ (km s^{-1})	$RV(\text{Si II } 6371 \text{ \AA})$ (km s^{-1})
ra5788	52721.3728	–29.71				
mj170023	52930.5671	25.36	21.45	21.11	18.65	20.07
mj170025	52930.6315	25.23	21.03	20.75	17.80	18.98
mk120038	52956.5608	16.02	21.45	21.67	17.67	20.76
ml090033	52983.4198	3.03	20.12	18.98	16.15	18.86
na050019	53010.4552	–11.13	13.55	15.33	14.84	16.80
na050021	53010.5053	–11.23	16.48	15.82	13.41	16.43
nd210018	53117.2973	–23.56	13.44	16.89	15.73	16.70
nd210019	53117.3210	–23.57	15.78	17.09	13.39	12.61
nd220014	53118.3330	–23.35	15.06	18.36	13.79	16.32
nd300002	53126.3175	–20.47	12.67	13.76	14.90	18.87
ng300048	53217.5797	21.00	18.70	10.85	15.09	18.95
ng300049	53217.5864	21.01	16.35	12.35	12.79	17.14
nh220044	53240.5571	27.37	15.60	13.35	14.20	13.74
nh220045	53240.5649	27.36	14.43	13.58	13.35	15.67
nh220049	53240.5862	27.35	15.00	14.95	12.49	14.69
nh220053	53240.6052	26.32	14.99	10.90	13.32	15.52
nh230063	53241.5625	27.55	12.98	14.95	13.63	17.10
ni020057	53251.6021	28.97	15.21	15.56	11.75	15.84
ni060034	53255.6179	28.14	11.90	11.14	9.90	14.66
ni080043	53257.5953	29.47	14.39	—	14.39	—
nj240062	53303.5864	23.00	11.76	10.54	9.57	12.05
nk240049	53334.5637	10.01	8.79	—	—	—
nl100020	53350.2773	2.36	13.55	11.30	9.52	11.50
oa160018	53387.3315	–16.40	12.44	12.31	10.18	11.89
oc220010	53452.3157	–29.61	10.35	10.01	6.21	5.04
oc310022	53461.3659	–28.62	10.47	10.03	6.91	10.42
od010015	53462.2998	–28.42	11.33	9.78	6.25	11.64
od010016	53462.3100	–28.41	10.15	10.12	5.51	10.18
oi060036	53620.5833	29.34	9.90	9.15	7.15	4.46
oi060037	53620.5954	29.33	9.30	11.79	8.23	10.97
oj070018	53651.4465	27.84	23.89	21.65	20.52	20.50
oj070028	53651.4953	27.79	23.28	21.63	21.83	23.74
oj070034	53651.5630	27.69	24.35	21.76	20.64	22.79
oj070040	53651.6182	27.58	23.69	21.45	19.95	21.99
oj070042	53651.6418	27.54	23.05	23.36	20.76	21.94
oj070044	53651.6703	27.48	25.93	24.46	21.79	23.70
oj080058	53652.4732	27.62	25.34	26.92	25.08	25.40
oj080062	53652.5220	27.56	23.91	23.42	21.44	23.02
oj080069	53652.5815	27.46	21.98	23.37	20.87	22.44
oj080073	53652.6229	27.38	24.64	28.68	25.40	23.28
oj080079	53652.6823	27.26	27.72	25.32	23.06	27.61
oj260033	53670.4313	21.60	26.45	24.66	19.67	23.76
oj260035	53670.4447	21.58	24.58	22.92	21.83	22.17
oj290036	53673.4859	20.51	25.52	22.75	20.12	21.90
oj290037	53673.5018	20.48	21.98	22.49	20.33	22.87
pa080032	53744.3096	–12.56	16.11	16.95	14.12	14.79
pj110024	54020.6019	26.67	11.60	11.71	9.29	12.49
qc160019	54176.2664	–29.87	9.03	10.00	5.16	8.53
qc160037	54176.3253	–29.98	8.83	10.50	6.73	7.65
qc160046	54176.4145	–30.04	9.94	9.52	6.06	8.80
qc270011	54187.3995	–29.25	8.95	10.44	5.00	7.82
qd020010	54193.3620	–28.37	7.03	10.44	4.54	7.95
qd070002	54198.3054	–27.40	9.50	10.71	6.31	8.86
qd130019	54204.2939	–26.03	8.63	9.98	3.03	7.47
qd130023	54204.3337	–26.05	9.20	9.15	5.43	4.80
qd140022	54205.3262	–25.79	9.31	9.81	5.81	8.30
qe020011	54223.3037	–20.03	13.92	—	—	—
qe020012	54223.3097	–20.03	11.02	12.46	2.89	6.97
qh240029	54337.5997	27.59	11.53	13.34	12.39	15.14
qh250033	54338.6177	27.71	11.84	11.91	9.87	13.95
qi150036	54359.5365	29.70	20.28	22.21	18.66	20.35
qi160031	54360.5360	29.70	20.50	22.06	19.61	23.03
qi160039	54360.6371	29.57	21.48	20.63	17.17	21.79
qj130036	54387.4787	26.51	21.26	18.68	21.17	20.95
qj130040	54387.5534	26.39	22.08	20.12	20.21	21.70
qj130046	54387.6826	26.13	23.03	21.13	19.13	21.96
rb250029	54522.3202	–28.60	17.53	16.29	15.33	17.04

Table A.3. Heliocentric radial velocities (RV) of HR 1847B – spectra from Ondřejov Observatory.

file	HJD (JD–2400000)	V_{hel} (km s ⁻¹)	$RV(H\alpha)$		
			(km s ⁻¹) wings	(km s ⁻¹) emission	(km s ⁻¹) absorption
ra5806	52721.8197	-29.59	11.10	9.73	14.30
mj170025	52930.6315	25.23	15.40	12.47	18.92
mk120038	52956.5608	16.02	15.05	12.71	19.70
nc290015	53094.3765	-28.89	14.39	13.21	17.90
nd300001	53126.3043	-20.50	18.17	16.41	18.17
nh220047	53240.5755	27.33	27.44	16.00	12.75
ni020058	53251.6217	27.36	7.47	6.88	9.22
ni130036	53262.5828	29.65	10.24	9.06	10.82
nj240060	53303.5565	23.02	3.83	-0.19	2.16
nj240061	53303.5692	22.99	8.58	7.40	7.99
oa160016	53387.3113	-16.39	19.80	8.08	18.92
od010017	53462.3213	-28.44	10.92	9.16	10.92
oi060038	53620.6195	29.30	21.00	18.06	24.51
oi220034	53636.6211	29.34	23.59	24.17	24.76
oi220035	53636.6365	29.31	17.11	20.04	23.52
oj070034	53651.5630	27.69	19.70	17.94	29.08
oj070040	53651.6182	27.58	12.55	-2.11	13.14
oj070042	53651.6418	27.54	21.86	30.69	21.89
oj070044	53651.6703	27.48	21.25	14.80	27.70
oj080060	53652.4977	27.60	—	37.52	24.62
oj280042	53672.5077	21.87	12.90	16.42	19.94
oj290035	53673.4623	21.60	11.50	7.39	—
pj110026	54020.6245	26.62	7.44	19.17	13.31
qc160019	54176.2664	-29.87	8.43	7.26	10.78
qc160039	54176.3427	-29.98	7.94	5.60	11.46
qc160048	54176.4353	-30.05	8.46	7.87	11.39
qc270010	54187.3763	-29.24	2.51	7.78	11.30
qd020011	54193.3770	-28.37	5.14	22.14	3.97
qd130021	54204.3139	-26.05	8.04	3.93	11.56
qd140024	54205.3461	-25.80	4.30	8.99	7.23
qh240030	54337.6245	27.57	20.89	32.61	23.23
qi150038	54359.5627	29.68	22.60	22.02	21.43
qi160033	54360.5562	29.68	23.68	37.17	24.27
qi160039	54360.6371	29.57	20.12	37.13	20.12
qj130046	54387.6826	26.13	22.66	32.04	23.25
rb250027	54522.2805	-28.54	8.89	—	—
rb250033	54522.3822	-28.73	8.21	—	—
rb250035	54522.4158	-28.77	7.35	—	—
rc220012	54548.3622	-29.65	21.58	—	—

Table A.4. Heliocentric radial velocities (RV) of HR 1847B – spectra from Rozhen Observatory.

file	HJD (JD–2400000)	V_{hel} (km s ⁻¹)	$RV(H\alpha)$		
			(km s ⁻¹) wings	(km s ⁻¹) emission	(km s ⁻¹) absorption
07h049	54341.5732	28.25	21.98	35.69	23.52
07h136	54342.6176	28.33	21.19	28.47	26.19
07h216	54343.5993	28.50	21.33	25.90	21.33